A chemical inhibitor of N-WASP reveals a new mechanism for targeting protein interactions

Jeffrey R. Peterson[†], R. Scott Lokey[†], Timothy J. Mitchison, and Marc W. Kirschner[‡]

Department of Cell Biology and the Institute for Chemistry and Cell Biology, Harvard Medical School, 240 Longwood Avenue, Boston, MA 02115

Cell morphology and motility are governed largely by complex signaling networks that ultimately engage the actin cytoskeleton. Understanding how individual circuits contribute to the process of forming cellular structures would be aided greatly by the availability of specific chemical inhibitors. We have used a novel chemical screen in *Xenopus* cell-free extracts to identify compounds that inhibit signaling pathways regulating actin polymerization. Here we report the results of a high-throughput screen for compounds that inhibit phosphatidylinositol 4,5-bisphosphate (PIP₂)-induced actin assembly and the identification of the first compound, a cyclic peptide, known to block actin assembly by inhibiting an upstream signaling component. We identify the target of this compound as N-WASP, a protein that has been investigated for its role as a node interconnecting various actin signaling networks. We show that this compound prevents activation of the Arp2/3 complex by N-WASP by allosterically stabilizing the autoinhibited conformation of N-WASP.

Biologists have long appreciated the use of specific chemical inhibitors to dissect complex signaling pathways. Only recently, however, has there been a concerted effort to apply combinatorial chemistry to the study of basic problems in cell biology. Termed ''chemical genetics'' to suggest an analogy with ''forward'' genetics in biology, the approach involves the screening of random chemical libraries for compounds that induce a particular phenotype of interest. Tracing the inhibitor (mutant) back to its target protein provides a causal link between the target and its associated phenotype.

One advantage of chemical genetics over traditional genetic approaches is that small molecules can be used to probe dynamic phenomena on a time scale that does not allow up- and down-regulation of compensatory genes. Changes in cell morphology, for example, are usually rapid and transient, making them difficult to study by genetic approaches and also difficult to model in cell-free systems. In fact, small molecule natural products (e.g., Taxol and cytochalasins) have been invaluable tools for elucidating the physiological roles of the cytoskeletal proteins actin and tubulin. But although actin and tubulin seem to be particularly vulnerable to chemical inhibitors, little has been reported on the use of small molecules to perturb the cytoskeleton upstream of the structural components themselves.

The actin cytoskeleton can be regulated by diverse extracellular cues and intracellular messengers including small rho-family GTPases, phosphoinositides, and calcium (1, 2). How these signals converge to promote temporally and spatially discrete structures has been a subject of intense interest. Work from several laboratories has now provided a framework model for the mechanism by which new actin filaments are generated at the plasma membrane of motile cells (3, 4). According to this model, diverse membrane-proximal signals can recruit and activate members of the Wiskott Aldrich Syndrome protein (WASP) family of proteins. This family of signal-integrating proteins in turn activates the Arp2/3 complex, a 220-kDa protein complex that directly promotes the rapid generation of new actin filaments (5).

Signaling pathways such as those that regulate actin assembly are governed largely by dynamic interactions between proteins.

Because protein–protein contacts are often mediated by residues spread over a large surface area (6, 7), they are generally considered resistant to inhibition by small molecules. We have been interested in the synthesis of combinatorial libraries that contain relatively large hydrophobic compounds, reasoning that such molecules would be capable of binding to diffuse hydrophobic surfaces, thereby enabling them to target protein–protein interactions more effectively than lower molecular weight compounds.

Cyclic peptides offer convenient scaffolds for the synthesis of libraries containing large complex structures, because size and complexity can be built up by adding amino acid monomers with little loss in overall yield. In addition, we reasoned that the same structural principles that underlie protein–protein interactions can be mimicked by using short polypeptides. But in contrast to linear peptides, cyclic peptides are stabilized against proteolytic degradation by exopeptidases. Furthermore, the structural rigidity imposed by cyclization may increase the affinity for targets by decreasing the entropic cost of peptide binding.

We have sought to identify cyclic peptides that specifically perturb components of a signaling pathway that generates new actin filaments. Cytoplasmic extracts provide a model system to recapitulate signaling to actin via WASP-family proteins and the Arp2/3 complex. When synthetic liposomes containing the phosphoinositide PIP₂ are added to cytoplasmic extracts of *Xenopus* eggs, actin is observed to polymerize on the vesicle surface (8). Some of the vesicles are propelled through the extract by a ''comet-like'' tail of filamentous actin much like that produced by the bacteria *Listeria monocytogenes* and *Shigella flexneri* in infected cells. We have shown that the actin polymerization depends on at least three endogenous proteins in the extract: the GTPase cdc42, N-WASP, and the Arp2/3 complex (8–10). These proteins interact directly to promote the rapid assembly of new actin filaments. In addition, as yet unknown factors link PIP₂ to cdc42 activation. Thus this assay seems to recapitulate the signaling pathways thought to operate at the plasma membrane. The polymerization of actin can be quantified by supplementing the extract with pyrene-labeled actin monomers. The fluorescence increases 20–30-fold on polymerization of pyrene-actin, thus providing a rapid and quantitative assay for actin assembly in a complex protein mixture.

By using this assay, a 14-aa cyclic peptide, 187-1, was identified that potently inhibited actin assembly induced by PIP₂. By using purified protein assays and photo-crosslinking, we demonstrate that 187-1 binds and inhibits N-WASP by an allosteric mechanism. This work validates N-WASP as a target for small molecule inhibitors and suggests a general mechanism for inhibition of

protein–protein interactions by the stabilization of preexisting autoinhibited conformations.

Materials and Methods

Synthesis of a 384-Member Library of Cyclic Peptides. Compounds were synthesized in parallel by using an IRORI microcan system. Peptides were elongated by using standard Fmoc chemistry with attachment to Rink amide TentaGel via the glutamine side chain as its C-terminal allyl ester. The loading of the resin was reduced to 0.14 mmol/g with a capping step by using *p*-tolylacetic acid before the addition of the Rink linker. Fmoc-Gln(NH-Rink resin)-OAll (10 g) was distributed into 384 IRORI microcans as a slurry in CH_2Cl_2 (100 ml). The cans were combined in a 1-liter filter flask and treated with 20% piperidine/*N,N*-dimethylacet-amide (DMA, 384 ml). After each addition of reagent or solvent, air bubbles were removed from the cans by the brief application of a slight vacuum to the flask. After stirring for 20 min, the cans were drained into a polypropylene salad spinner obtained from a local hardware store, and the solvent was removed by manual centrifugation. The cans were rinsed with DMA (2×400 ml), MeOH (2×400 ml), and DMA (2×400 ml). After each solvent treatment a vacuum was applied as described, and the cans were swirled vigorously for 2 min and drained by using the salad spinner. Couplings were performed in plastic bottles by using 0.075 M Fmoc-amino acid, 0.075 *O*-(benzotriazol-1-yl)-*N,N,N′,N′*-tetramethyluronium hexafluorophosphate, and 1.125 M diisopropylethylamine in DMA at 1.0 ml of solution/can. Each coupling was performed for 3 h with agitation. After the addition of the final lysine residue but before piperidine treatment, the cans were rinsed with CH_2Cl_2 and purged with argon in a 1-liter flask. A degassed solution of $Pd(Ph_3P)_4$ (15 g) in $CHCl_3$/AcOH/*N*-methylmorpholine (37:2:1) was added to the cans under argon, and the cans were agitated overnight. The N-terminal Fmoc group was removed, and the cyclization was performed with a mixture of PyBop (15 g, 28.8 mmol), 1-hydroxyazabenztriazole (HOAT, 3.9 g, 28.8 mmol), and diisopropylethyl amine (7.5 ml, 43 mmol) in DMA (0.077 M). The cans were rinsed extensively with DMA, MeOH, and CH_2Cl_2 and archived. The compounds were cleaved from the resin by using the IRORI cleavage station (3:2 trifluoroacetic acid/CH_2Cl_2 with 2.5% triisopropylsilane, 3 ml each can, 3 h) and filtered into separate glass vials. The solvent was removed by using a rotary concentrator, and the residue was triturated with ether. The resulting ether suspension was packed down by centrifugation, the ether was decanted, and the samples were allowed to air dry. The remaining white solid was taken up in DMSO (200 μl), and each sample was diluted 1:10 into acetonitrile and analyzed by liquid chromatography/MS [HPLC gradient, 75% to 45% 0.1% formic acid/H_2O to 0.1% formic acid/CH_3CN; column, Symmetry C_{18} (Waters), 3.5 μm, 2.1 $\times$ 50 mm; column temp, 60°C].

Structural Confirmation of 187-1. Liquid chromatography/MS analysis of the active well (electrospray ionization in the positive mode) showed peaks in the chromatogram corresponding to both cyclomonomer ([M+H]$^+$ = 892.3) and cyclodimer ([M+H]$^+$ = 1784.6; [M+2H] (2+) = 892.3). The ratio of monomer/dimer was $\approx$6:1 by integration. The first ^{13}C isotope peak for cyclomonomer appeared at *m/z* 893.3, whereas that of the doubly charged cyclodimer appeared at *m/z* 892.8. The cyclodimer was resynthesized independently by solid-phase peptide synthesis of the corresponding linear 14-mer precursor followed by cyclization. This material was identical to the cyclodimer contained in the original synthesis well by HPLC retention time and mass spectrometric analysis.

Pyrene-Actin Assembly Assay in *Xenopus* Cytoplasmic Extracts. *Xenopus* CSF-arrested egg extracts were prepared as described (11) and were then diluted 5-fold with CSF-XB (11) containing 1 mM

dithiothreitol, 10 μg/ml each of chymostatin, leupeptin, and pepstatin and 1/100 volume of CSF-Energy mix (11). The dilute extract was centrifuged for 3 h in a Ti45 rotor at 35,000 rpm. The supernatant was recentrifuged from 1–3 h in an SW28 rotor at 26–27,000 rpm, and the resulting extract was aliquoted and frozen. Before use, the extracts were diluted 1:1 with 0.2 mM ATP/CSF-XB, and actin was added to 2.8 μM [50% pyrene-labeled, prepared from rabbit muscle as described (8)]. Then 30 μl of extract was aliquoted per well in 384-well plates maintained at 4°C. Approximately 200 nl of each compound was transferred individually into each well by using polypropylene pin arrays (Genetix, Dorset, United Kingdom). Subsequently, PIP$_2$-containing liposomes (PIP$_2$/phospatidylcholine/phosphatidyl-inositol, 4:48:48 molar ratio at $\approx$15 μM final concentration total lipid) were added by pin transfer. The plate was transferred to a Wallac plate reader and fluorescence (excitation, 355 nm; emission, 410 nm) was measured every $\approx$1 min for $\approx$25 min at room temperature.

Visual Assay for Rhodamine-Actin Assembly. CSF-arrested egg extract was diluted with an equal volume of 0.2 mM ATP/CSF-XB, and rhodamine-labeled monomeric actin (Cytoskeleton, Denver) was added to a final concentration of 38 μg/ml. DMSO or 46 μM 187-1 (final concentration) was added, and PIP$_2$-containing liposomes (185 μM final) or verprolin, cofilin, acidic domain-containing region of N-WASP (VCA) polypeptide (13 μg/ml final) were added to initiate assembly. Reaction mixtures were pressed between cover glasses and imaged on a Zeiss Axiovert.

Pure Protein Actin Polymerization Assay. Thirty-microliter reactions in 384-well plates were prepared at 4°C in 0.2 mM ATP/CSF-XB. Reaction components were used at the following concentrations: 45–75 nM Arp2/3 complex, 5.5 μg/ml VCA, 240 nM N-WASP, and 80 nM GST-cdc42. Arp2/3 was purified from bovine brain cytosol by sequential chromatography on butyl Sepharose, DEAE Sepharose, and GST-VCA agarose. Untagged recombinant rat N-WASP protein was expressed in Sf9 cells and purified as described (10). Recombinant cdc42 was purified as a GST fusion protein from Sf9 cell membranes and was thrombin cleaved as described (9). VCA was purified as a GST fusion protein and cleaved as described (10). Actin (2.4 μM final, 20% pyrene-labeled) was added last, and the time course of polymerization was measured as described above.

Photo-Crosslinking of a Biotinylated Derivative of 187-1 Containing a Benzoylphenylalanine [187-1(Bpa)*]. Reaction mixtures containing 200 nM each of actin, N-WASP, and Arp2/3 in CSF-XB were photo-crosslinked for 5 min at 4°C under UV light (365 nm, 13 mW/cm^2).

N-/C-Terminal N-WASP Binding Assay. Fifty-microliter pull-down assay reactions consisted of CSF-XB/0.1% Tween 20/1 mM DTT/0.5 M NaCl/2 mg/ml chicken lysozyme containing 10 μg of GST-VCA immobilized on glutathione agarose, 2.4 μM HT-WGP prepared as described (12), and 13 μM cdc42 purified as a GST-fusion protein from *E. coli* and thrombin-cleaved. The cdc42 was charged with GTPγS by incubation for 25 min at 30°C in 2 mM EDTA/0.2 mM GTPγS followed by the addition of MgCl$_2$ to 5 mM on ice. After 1 h of incubation at room temperature, the beads were washed twice with CSF-XB/0.1% Tween 20/1 mM DTT and resuspended in sample buffer for SDS/PAGE and Western blotting with anti-His$_5$ antibodies (Qiagen, Chatsworth, CA).

Results and Discussion

Individual library compounds were transferred by pin array into assay wells containing *Xenopus* egg cytoplasmic extract and pyrene-labeled actin. A signal to induce actin assembly was

Table 1. Structural representation of the eight sublibraries of cyclic peptides screened

cyclo(D,LLys-D,LPhe-D,LPhe-D,LPhe-D,LPro-LGln)
cyclo(D,LLys-D,LPhe-D,LPhe-D,LPro-D,LPro-LGln)
cyclo(D,LLys-D,LPhe-D,LPro-D,LPhe-D,LPro-LGln)
cyclo(D,LLys-D,LPro-D,LPhe-D,LPhe-D,LPro-LGln)
cyclo(D,LLys-D,LPhe-D,LPhe-D,LPhe-D,LPro-D,LPro-LGln)
cyclo(D,LLys-D,LPhe-D,LPhe-D,LPro-D,LPhe-D,LPro-LGln)
cyclo(D,LLys-D,LPhe-D,LPro-D,LPhe-D,LPhe-D,LPro-LGln)
cyclo(D,LLys-D,LPro-D,LPhe-D,LPro-D,LPhe-D,LPro-LGln)

provided by a second pin transfer of PIP$_2$-containing liposomes. We have shown previously that PIP$_2$ induces actin assembly in a manner that depends on an endogenous signaling pathway that is present in the extract (8–10). The increase in pyrene fluorescence in each well was then monitored as a function of time, reflecting the actin polymerization kinetics in the extract.

By using this assay we were able to screen a collection of over 26,000 compounds from multiple sources and identified ≈200 compounds that completely inhibited net actin assembly at the screening concentration of ≈60 μM. These molecules included both traditional "drug-like" small molecules and cyclic peptides. Among the compounds that exhibited the greatest potency in both primary and secondary assays (see below, other active compounds will be reported elsewhere) was a member of a library of cyclic peptide "scaffolds" containing the amino acids Phe, Pro, Gln, and Lys. This library was designed as a set of eight geometrically diverse hexa- and heptapeptide sublibraries categorized by ring size and Pro position. Within each sublibrary all possible diastereomers (excluding enantiomers) were included, yielding a total of 384 members (Table 1).

Liquid chromatography/MS analysis of the active well revealed the presence of two related cyclic peptides: a cyclic heptapeptide of the sequence L-Lys–D-Phe–D-Pro–D-Phe–L-Phe–D-Pro–L-Gln as well as the corresponding cyclodimeric species at a molar ratio of ≈6:1. On resynthesis and purification, the cyclomonomer had no effect at up to 100 μM on PIP$_2$-stimulated actin assembly in *Xenopus* extract (data not shown). By contrast, the 14-residue cyclodimer, called 187-1 (Table 2), showed a dose-dependent inhibition of PIP$_2$-stimulated actin assembly with an IC$_{50}$ of ≈2 μM (estimated as the concentration of peptide required to inhibit the slope of the elongation phase of actin polymerization by 50%; Fig. 1a). A derivative of 187-1, 187-F$_2$ΔA$_2$, in which two phenylalanine residues were replaced by alanine residues with identical stereochemistry (Table 2), was inactive even at 20 μM (data not shown).

To confirm that the inhibition by 187-1 was not simply caused by a quenching of pyrene fluorescence, we visualized microscopically the polymerization of actin in response to PIP$_2$ by adding rhodamine-labeled actin monomers to the extract. Although total rhodamine fluorescence remains the same in this assay, localized densities of newly formed actin filaments can be observed as discrete foci of bright rhodamine staining against a darker background (8). Indeed, pretreatment of extract with

Table 2. Amino acid sequence of cyclic peptides used in this study

187-1:	cyclo(LLys-DPhe-DPro-DPhe-LPhe-DPro-LGln)$_2$
187-1(F$_2$ΔA$_2$):	cyclo(LLys-DPhe-DPro-DPhe-LALa-DPro-LGln)$_2$
187-1(Bpa)*:	cyclo(LLys(biotin)-DPhe-DPro-DPhe-LBpa-DPro-LGln-LLys-DPhe-DPro-DPhe-LPhe-DPro-LGln)
187-1(Bpa):	cyclo(LLys-DPhe-DPro-DPhe-LBpa-DPro-LGln-LLys-DPhe-DPro-DPhe-LPhe-DPro-LGln)
F12:	cyclo(LLys-DPhe-DPro-LPhe-DPhe-LPro-LGln)$_2$
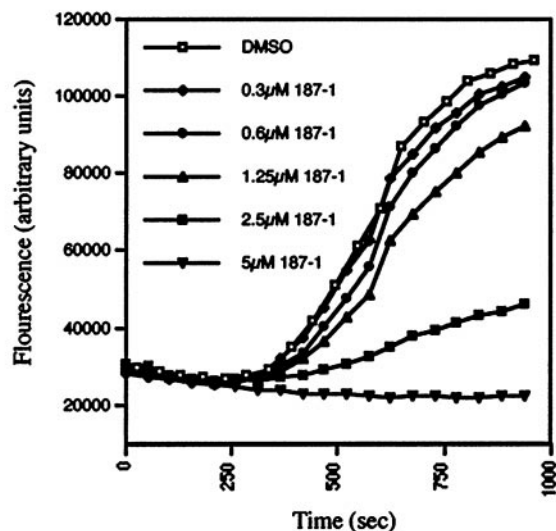
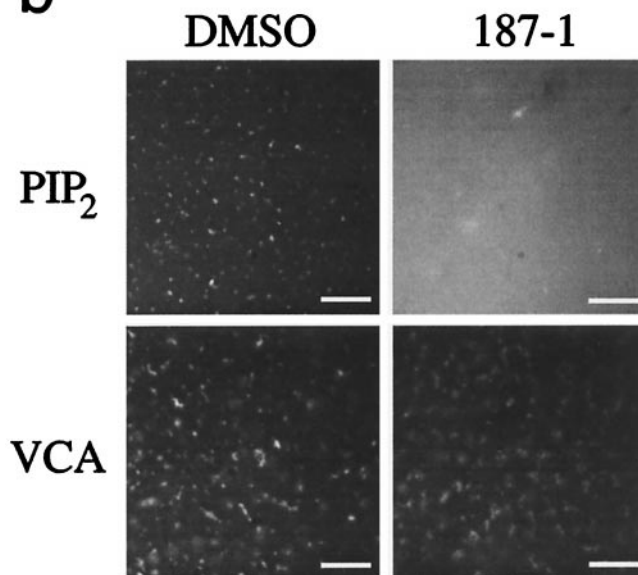**Fig. 1.** 187-1, a 14-amino acid cyclic peptide, inhibits PIP$_2$-induced but not VCA-induced actin assembly in *Xenopus* cytoplasmic extract. (*a*) Polymerization kinetics of pyrene-actin after the addition of PIP$_2$-containing liposomes into extract containing the indicated concentrations of 187-1. (*b*) Immunofluorescence images of rhodamine-actin in extract ± 46 μM 187-1 induced to polymerize by PIP$_2$-containing liposomes (*Upper*) or 0.5 μM VCA polypeptide (*Lower*). (Scale bars, 100 μm.)

187-1 prevented the appearance of actin foci as compared with pretreatment with solvent alone (Fig. 1b Upper).

To determine how 187-1 inhibited actin polymerization, we tested whether 187-1 could inhibit polymerization in extracts initiated by factors that act downstream of PIP$_2$. The assembly of new actin filaments in extract depends on the actin-nucleating activity of the Arp2/3 complex (9). As shown in Fig. 2a, PIP$_2$ activates actin assembly by Arp2/3 via at least two other signaling proteins, the small GTP-binding protein cdc42 and N-WASP, a ubiquitously expressed relative of WASP (10). The primary role of PIP$_2$ in the pathway may be to activate GTP/GDP nucleotide exchange on cdc42 (12).
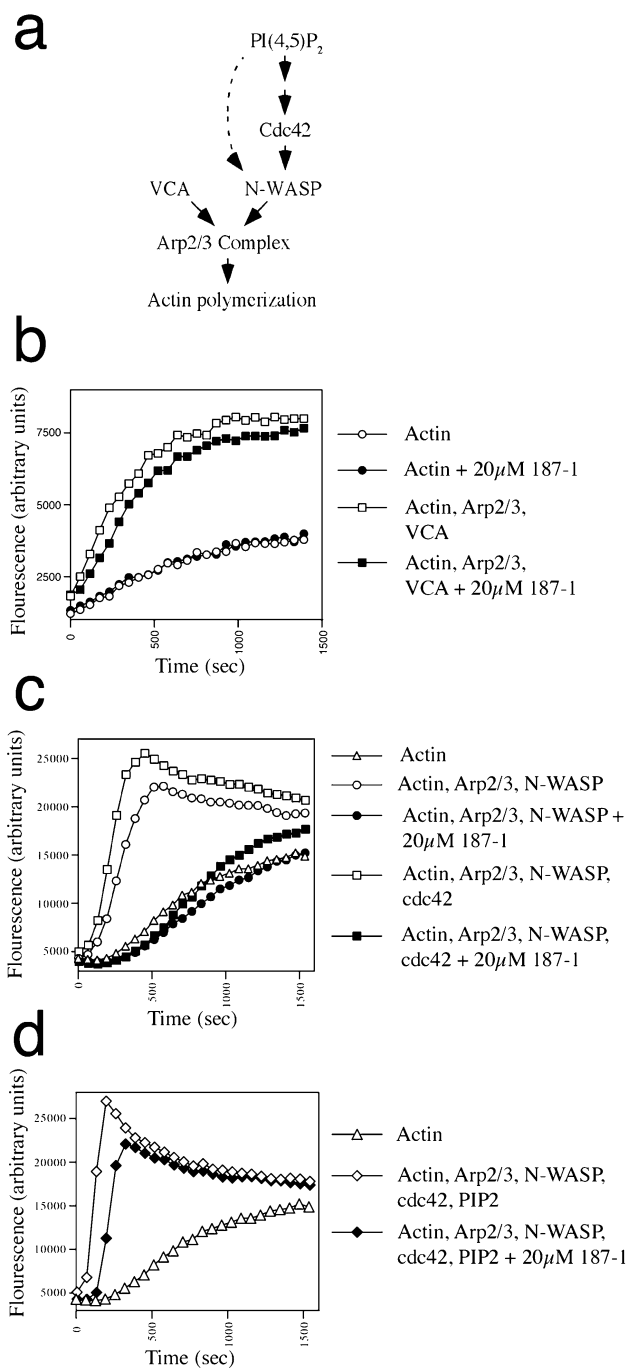
a

PI(4,5)P$_2$

Cdc42

VCA   N-WASP

Arp2/3 Complex

Actin polymerization

b

Fluorescence (arbitrary units) vs Time (sec)

- ○ Actin
- ● Actin + 20μM 187-1
- □ Actin, Arp2/3, VCA
- ■ Actin, Arp2/3, VCA + 20μM 187-1

c

Fluorescence (arbitrary units) vs Time (sec)

- △ Actin
- ○ Actin, Arp2/3, N-WASP
- ● Actin, Arp2/3, N-WASP + 20μM 187-1
- □ Actin, Arp2/3, N-WASP, cdc42
- ■ Actin, Arp2/3, N-WASP, cdc42 + 20μM 187-1

d

Fluorescence (arbitrary units) vs Time (sec)

- △ Actin
- ◇ Actin, Arp2/3, N-WASP, cdc42, PIP2
- ◆ Actin, Arp2/3, N-WASP, cdc42, PIP2 + 20μM 187-1

Fig. 2. 187-1 inhibits N-WASP activation of the Arp2/3 complex. (*a*) Schematic of the known components involved in signaling from PIP$_2$ to actin in *Xenopus* extract and their sequence of action. Note that PIP$_2$ has a primary role upstream of cdc42 but can also bind directly to and promote activation of N-WASP. (*b–d*) Pyrene-actin polymerization kinetics in the presence of the indicated purified components. (*b*) 187-1 does not affect actin polymerization downstream of VCA. (*c*) N-WASP-stimulated actin polymerization is inhibited by 187-1. (*d*) N-WASP activated by both cdc42 and PIP2-containing liposomes is resistant to inhibition by 187-1.

Signaling to Arp2/3 can be short-circuited experimentally, bypassing the need for factors upstream of Arp2/3, by a C-terminal peptide derived from N-WASP. This peptide (amino acids 392–505) has been termed "VCA" for sequence domains showing homology to *v*erprolin, *c*ofilin, and an *a*cid stretch of amino acids (13). This polypeptide is itself a potent dominant

activator of the Arp2/3 complex (see Fig. 2*a* and ref. 10). Pretreatment of extract with 187-1, however, did not prevent the VCA fragment from inducing foci of new actin filaments (Fig. 1*b Lower*). Thus 187-1 does not directly inhibit the polymerization of actin, nor does it affect the ability of the Arp2/3 complex to nucleate new actin filaments. These experiments indicate that 187-1 specifically targets a component in the signaling pathway from PIP$_2$ to the Arp2/3 complex.

To identify the molecular target of 187-1, we used a reconstituted actin assembly reaction consisting of purified proteins in buffer to test the two known candidate protein targets, cdc42 and N-WASP. As in the extract-based assay, the formation of actin polymer was monitored by the increase in pyrene-actin fluorescence. In the presence of high salt and ATP the polymerization of actin occurs spontaneously; however, when the Arp2/3 complex and the VCA fragment of N-WASP are included in the reaction, the kinetics of assembly are greatly stimulated (Fig. 2*b*, VCA; ref. 10). Confirming our results in extract, 187-1 had no effect on either the slow polymerization kinetics of actin alone or on the accelerated kinetics in the presence of the Arp2/3 complex and VCA (Fig. 2*b*).

N-WASP has a modest Arp2/3-stimulating activity *in vitro*, which can be further activated by cdc42 bound to the nonhydrolyzable GTP analogue GTPγS (Fig. 2*c*, compare Actin, Arp2/3, and N-WASP ± cdc42; ref. 10). We monitored the polymerization kinetics of pyrene-actin in the presence or absence of pure Arp2/3 complex, N-WASP, GTPγS-cdc42, and the inhibitor 187-1. In all reactions containing 187-1, actin polymerization kinetics were slowed to a rate comparable with that observed for actin alone (Fig. 2*c*). This suggests that 187-1 antagonized the filament-nucleating activity of Arp2/3-N-WASP-cdc42 and that actin merely polymerized at its default rate. Similar to its potency in extract, 187-1 was effective in the pure protein assay at concentrations below 10 μM (data not shown).

As a control, we synthesized and purified the enantiomer of 187-1. It had no effect on N-WASP-containing polymerization reactions at concentrations >50 μM (data not shown). Because inhibition by 187-1 was observed even in the reaction without cdc42, cdc42 does not seem to be the target of 187-1. Taken together with the observation that 187-1 does not inhibit the Arp2/3 complex (Fig. 2*b*), this experiment suggests that 187-1 directly inhibits both the moderate basal activity of N-WASP as well as cdc42-activated N-WASP. In addition, the essential role of N-WASP in PIP$_2$-induced actin assembly in extract (10) and the comparable potency of 187-1 both in the extract and at inhibiting N-WASP activity in the pure protein assay suggest that inhibition of N-WASP is responsible for the loss of actin assembly in extract.

The activation of N-WASP by cdc42 can be potentiated by direct binding of PIP$_2$ to a basic region in the N-terminal regulatory domain of N-WASP (12, 14). We have shown that this interaction is not required for actin assembly induced by PIP$_2$ in *Xenopus* extract and therefore concluded that the predominant role of PIP$_2$ in this pathway is the upstream activation of cdc42 (12). Nevertheless, we tested the effect of 187-1 on cdc42 and PIP$_2$ coactivation of N-WASP by using the purified protein assay. Interestingly, 187-1 was significantly less potent against N-WASP activated by both cdc42 *and* PIP$_2$ (Fig. 2*d*). This decrease in potency was not caused by lipid sequestration of 187-1, because liposomes lacking PIP$_2$ did not affect the potency of 187-1 against cdc42-activated N-WASP (data not shown). Most likely, the potent cooperativity of the activation of N-WASP by both cdc42 and PIP$_2$ (14) explains the reduced potency of 187-1 to inhibit N-WASP in the presence of both activators.

To test whether 187-1 directly binds to N-WASP, we synthesized a biotinylated derivative of 187-1 containing a benzoyl-phenylalanine photo-crosslinking group. This compound [187-
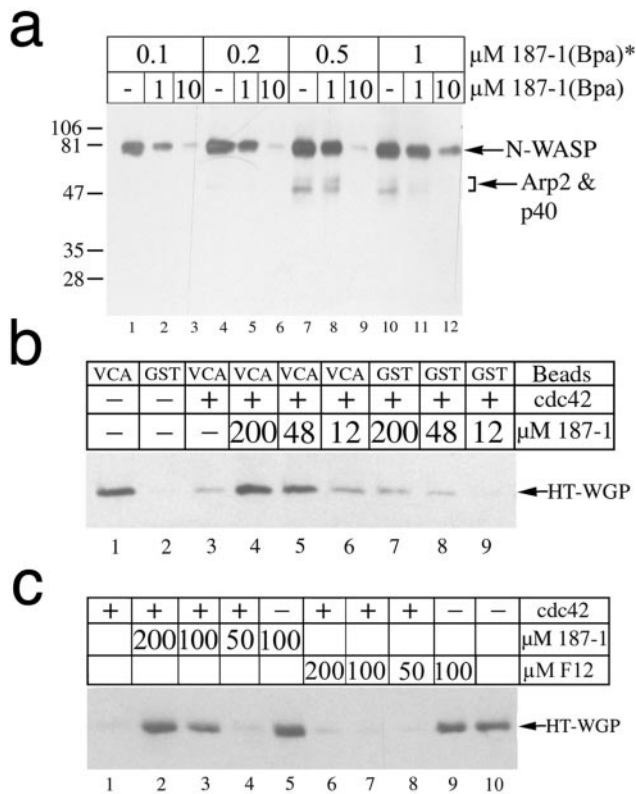
a

	0.1			0.2			0.5			1			μM 187-1(Bpa)*
	−	1	10	−	1	10	−	1	10	−	1	10	μM 187-1(Bpa)

106 —
81 — ← N-WASP
47 —]← Arp2 & p40
35 —
28 —

Lanes: 1 2 3 4 5 6 7 8 9 10 11 12

b

VCA	GST	VCA	VCA	VCA	VCA	GST	GST	GST	Beads
−	−	+	+	+	+	+	+	+	cdc42
−	−	−	200	48	12	200	48	12	μM 187-1

←HT-WGP

Lanes: 1 2 3 4 5 6 7 8 9

c

+	+	+	+	−	+	+	+	−	−	cdc42
200	100	50	100							μM 187-1
					200	100	50	100		μM F12

←HT-WGP

Lanes: 1 2 3 4 5 6 7 8 9 10

Fig. 3. 187-1 binds to N-WASP and stabilizes the autoinhibited conformation. (*a*) 187-1 photo-crosslinks predominantly to N-WASP. A biotinylated photo-crosslinkable derivative of 187-1, 187-1(Bpa)* (Fig 1*a*) was incubated with an equimolar mixture of actin, the Arp2/3 complex, and N-WASP and was crosslinked by UV illumination. In some reactions (lanes 2, 3,5, 6, 8, 9, 11, and 12), we included a nonbiotinylated competitor, 187-1(Bpa) (Fig 1*a*). The concentrations of 187-1(Bpa)* and 187-1(Bpa) used are indicated. Reactions were analyzed by SDS/PAGE/Western blotting, and biotin was detected by using horseradish peroxidase-streptavidin and chemiluminescence. (*b*) 187-1 stabilizes the autoinhibited conformation of N-WASP. GST alone or GST-VCA fusion proteins were immobilized on glutathione agarose and incubated with the His$_6$-tagged WGP fragment of N-WASP (HT-WGP, amino acids 1–396) in the presence of GTPγS-bound cdc42 and 187-1 as indicated. After washing, the bound material was eluted in SDS/PAGE sample buffer, and HT-WGP was detected by SDS/PAGE/Western blotting by using anti-His antibodies and chemiluminescent detection. (*c*) 187-1 but not a diastereomer, F12, stabilizes N-WASP. GST-VCA-coated beads were incubated with HT-WGP as shown in *b* in the presence or absence of the indicated components, and bound HT-WGP was detected as described above.

1(Bpa)*] and a nonbiotinylated competitor [187-1(Bpa)] both retained inhibitory activity in extract (IC$_{50}$ values of ≈3.75 μM; data not shown). We incubated 187-1(Bpa)* with an equimolar mixture (200 nM each) of actin, the Arp2/3 complex, and N-WASP and photo-crosslinked them by UV illumination. The mixture was then analyzed by SDS/PAGE/Western blotting, and the proteins that were crosslinked by 187-1(Bpa)* were identified by chemiluminescent detection of biotin by using streptavidin-horseradish peroxidase. Fig. 3*a* shows that 187-1(Bpa)* crosslinked prominently to N-WASP and to a much lesser degree to the Arp2 and p40 subunits of the Arp2/3 complex. No crosslinking was observed to actin even when incubated alone with 187-1(Bpa)* (data not shown). Importantly, the crosslinking of N-WASP to 187-1(Bpa)* could be competed by excess 187-1(Bpa) (Fig. 3*a*), indicating a specific and limiting binding site. Furthermore, crosslinking to N-WASP did not require the presence of Arp2/3 or actin (data not shown). When it was UV-irradiated in *Xenopus* extract, however, 187-
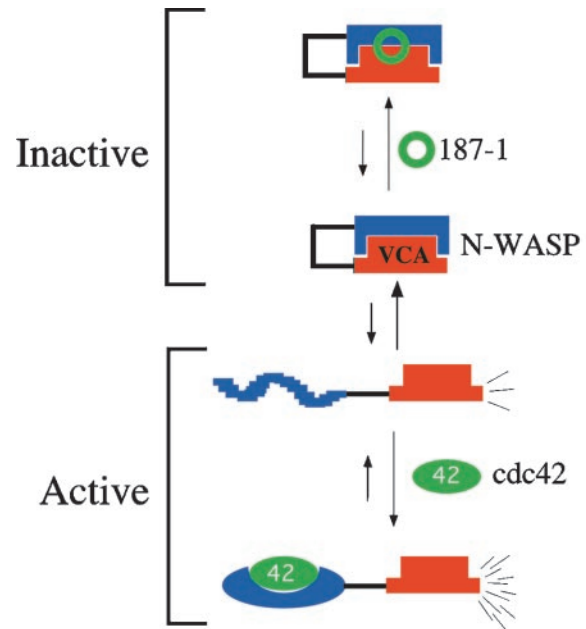
1(Bpa)* crosslinked to a number of protein bands (data not shown), suggesting that 187-1 may also interact with other proteins in the extract.

N-WASP consists of an N-terminal regulatory domain, a Pro-rich "hinge" segment, and the C-terminal VCA domain, responsible for activation of the Arp2/3 complex (15, 16). In the native structure of the highly related WASP protein, the VCA domain packs closely against the *G* protein *b*inding *d*omain (GBD) of the N terminus of WASP (17). The interaction of the regulatory and activation domains suppresses the activation of Arp2/3 by the VCA peptide (12, 14, 18). In addition to VCA, however, the GBD of N-WASP binds to cdc42 (19). The consequence of this binding is a conformational change in the GBD that releases the VCA domain, enabling Arp2/3 activation (12, 14). Fig. 4 illustrates this model of the competition between cdc42 and VCA for binding to the GBD.

We hypothesized that 187-1 might act by stabilizing the regulatory–VCA intramolecular interaction, thus preventing Arp2/3 activation. To test this directly, we immobilized the VCA peptide as a GST-fusion protein on glutathione beads and incubated the beads with recombinant His$_6$-tagged N-terminal fragment of N-WASP (HT-WGP). After incubation, the beads were washed, and associated HT-WGP was detected by SDS-PAGE and Western blotting. As shown previously (12), HT-WGP could be recovered associated with the VCA beads in a manner that could be competed away by the inclusion of GTPγS-cdc42 in the reaction (Fig. 3*b*, lanes 1 and 3 and Fig. 3*c*, lanes 1 and 10). However, in a dose-dependent manner 187-1 but not F12 a diastereomer of 187-1, prevented the dissociation of HT-WGP from VCA by cdc42 (Fig. 3*c*, lanes 2–3 and 6–8, respectively). HT-WGP did not significantly associate with control GST-bound beads regardless of the presence of 187-1 (Fig. 3*b*, lanes 2 and 7–9). Thus we concluded that 187-1 prevents the activation of Arp2/3 by N-WASP by stabilizing the autoinhibitory binding of the N and C termini of N-WASP, preventing exposure of the VCA domain (Fig. 4). Structural work on the complex will be required to determine whether 187-1 inhibits by

Inactive / Active model

Fig. 4. A model for the inhibition of N-WASP by 187-1. Native N-WASP exists predominantly in a "closed" inactive conformation. Whereas binding to cdc42 stabilizes the "open" active conformation, 187-1 stabilizes the autoinhibited state. Competitive binding of 187-1 and cdc42 to N-WASP, therefore, drives the equilibrium between autoinhibited and activated states, respectively.

binding the regulatory domain–VCA interface or by stabilizing the VCA-binding conformation of WGP (17).

This work establishes the feasibility of regulating signaling through N-WASP by using a chemical inhibitor to stabilize the native, autoinhibited state. N-WASP itself is thought to integrate upstream signals from numerous sources and to transmit the signal to the Arp2/3 complex. Signals from receptor tyrosine kinases, viral and bacterial surface proteins SH3 domain-containing adaptor proteins, small GTPases, and phosphoinositides have all been shown to impinge on N-WASP (10, 13, 20–22). The identification of N-WASP as the target of a broad small molecule screen suggests that signaling through N-WASP is an important and rate-limiting step in the pathway from PIP_2 to actin. We are now poised to investigate the physiological consequences of disrupting this important signaling protein in an acute manner.

In addition to its normal role, N-WASP plays an important role in several pathological processes. Both the smallpox virus-related *Vaccinia* virus and the bacterial pathogen *S. flexneri* are intracellular parasites that directly recruit and activate N-WASP on their surfaces as an obligatory step in the spread of infection (20, 21). Furthermore, a novel clinical syndrome, X-linked severe congenital neutropenia, was shown recently to be caused by a destabilizing mutation in the GBD of WASP (L270P), resulting in a constitutively active protein (23). Thus, compounds that stabilize the inhibited conformation of N-WASP could be therapeutically useful. The lack of broad cellular lethality in N-WASP knockout mice (S. Snapper, personal communication) suggests that acute inhibition of N-WASP might be tolerated physiologically.

More broadly, the mechanism of inhibition by 187-1 identified here suggests a general principle for selecting proteins as targets of screens for chemical inhibitors. Native N-WASP is thought to exist in a dynamic equilibrium between an active, open confor-mation stabilized by the GBD–cdc42 intermolecular interaction and an autoinhibited, closed conformation stabilized by the GBD–VCA intramolecular interaction. Thus, regulation of N-WASP activity is mediated by the conformational plasticity of the GBD. The consequence of stabilizing the autoinhibited conformation of N-WASP is to prevent a productive interaction with the Arp2/3 complex. This finely tuned thermodynamic balance provides a locus both for cellular regulation and for potential perturbation by small molecules. Energetically small changes induced by compound binding could tip this balance in a particular direction. Although the cyclic peptide library used in this study was designed to generate large structures that could inhibit protein–protein interactions competitively, we serendipitously discovered a compound that inhibits a protein–protein interaction (that between N-WASP and Arp2/3) by an unexpected mechanism. The ability to identify allosteric small molecule inhibitors that bias conformational equilibria may prove generally easier than, for example, competing rigid-body protein–protein interactions with small molecules. Therefore, proteins that are known to exist in multiple conformations in equilibrium may be more amenable to chemical inhibition. Examples of such proteins include CREB and p21[Waf1/Cip1/Sdi1], and analysis of genomic sequences suggest that regulation by induced folding may not be uncommon (24).

1. Hall, A. (1998) *Science* **279,** 509–514.
2. Janmey, P. A. (1994) *Annu. Rev. Physiol.* **56,** 169–191.
3. Mullins, R. D. (2000) *Curr. Opin. Cell Biol.* **12,** 91–96.
4. Pantaloni, D., Le Clainche, C. & Carlier, M. F. (2001) *Science* **292,** 1502–1506.
5. Mullins, R. D. & Pollard, T. D. (1999) *Curr. Opin. Struct. Biol.* **9,** 244–249.
6. Jones, S. & Thornton, J. M. (1996) *Proc. Natl. Acad. Sci. USA* **93,** 13–20.
7. Stites, W. E. (1997) *Chem. Rev.* **97,** 1233–1250.
8. Ma, L., Cantley, L. C., Janmey, P. A. & Kirschner, M. W. (1998) *J. Cell Biol.* **140,** 1125–1136.
9. Ma, L., Rohatgi, R. & Kirschner, M. W. (1998) *Proc. Natl. Acad. Sci. USA* **95,** 15362–15367.
10. Rohatgi, R., Ma, L., Miki, H., Lopez, M., Kirchhausen, T., Takenawa, T. & Kirschner, M. W. (1999) *Cell* **97,** 221–231.
11. Desai, A., Murray, A., Mitchison, T. J. & Walczak, C. E. (1999) *Methods Cell Biol.* **61,** 385–412.
12. Rohatgi, R., Ho, H. Y. & Kirschner, M. W. (2000) *J. Cell Biol.* **150,** 1299–1310.
13. Miki, H., Miura, K. & Takenawa, T. (1996) *EMBO J.* **15,** 5326–5335.
14. Prehoda, K. E., Scott, J. A., Mullins, R. D. & Lim, W. A. (2000) *Science* **290,** 801–806.
15. Takenawa, T. & Miki, H. (2001) *J. Cell Sci.* **114,** 1801–1809.
16. Zigmond, S. H. (2000) *J. Cell Biol.* **150,** 117–120.
17. Kim, A. S., Kakalis, L. T., Abdul-Manan, N., Liu, G. A. & Rosen, M. K. (2000) *Nature (London)* **404,** 151–158.
18. Higgs, H. N. & Pollard, T. D. (2000) *J. Cell Biol.* **150,** 1311–1320.
19. Miki, H., Sasaki, T., Takai, Y. & Takenawa, T. (1998) *Nature (London)* **391,** 93–96.
20. Frischknecht, F., Moreau, V., Rottger, S., Gonfloni, S., Reckmann, I., Superti-Furga, G. & Way, M. (1999) *Nature (London)* **401,** 926–929.
21. Egile, C., Loisel, T. P., Laurent, V., Li, R., Pantaloni, D., Sansonetti, P. J. & Carlier, M. F. (1999) *J. Cell Biol.* **146,** 1319–1332.
22. Carlier, M. F., Nioche, P., Broutin-L'Hermite, I., Boujemaa, R., Le Clainche, C., Egile, C., Garbay, C., Ducruix, A., Sansonetti, P. & Pantaloni, D. (2000) *J. Biol. Chem.* **275,** 21946–21952.
23. Devriendt, K., Kim, A. S., Mathijs, G., Frints, S. G., Schwartz, M., Van Den Oord, J. J., Verhoef, G. E., Boogaerts, M. A., Fryns, J. P., You, D., Rosen, M. K. & Vandenberghe, P. (2001) *Nat. Genet.* **27,** 313–317.
24. Wright, P. E. & Dyson, H. J. (1999) *J. Mol. Biol.* **293,** 321–331.